Separation Science and Technology
Publication details, including instructions for authors and subscription information:
http://www.informaworld.com/smpp/title~content=t713708471

Separation of Gases by Pressure Swin

R. V. Jasra[a]; N. V. Choudary[a]; S. G. T. Bhat[a]
[a] Research Centre Indian Petrochemicals Corporation Limited, Vadodara, India

To cite this Article Jasra, R. V. , Choudary, N. V. and Bhat, S. G. T.(1991) 'Separation of Gases by Pressure Swin', Separation Science and Technology, 26: 7, 885 — 930
To link to this Article: DOI: 10.1080/01496399108050504
URL: http://dx.doi.org/10.1080/01496399108050504

SEPARATION SCIENCE AND TECHNOLOGY, 26(7), pp. 885–930, 1991

REVIEW

Separation of Gases by Pressure Swing Adsorption

R. V. JASRA, N. V. CHOUDARY, and S. G. T. BHAT
RESEARCH CENTRE
INDIAN PETROCHEMICALS CORPORATION LIMITED
VADODARA 391346, INDIA

Abstract

The recent status of pressure swing adsorption (PSA) as a process for separating multicomponent gas mixtures is reviewed. The applications of a new generation of adsorbents, such as zeolites, carbon molecular sieves, and, more recently, pore engineered molecular sieves, are described in detail. The more important theories of adsorption from gas mixtures as well as those of the PSA process are described briefly. The commercial applications of PSA the process—present and potential—are discussed at length.

INTRODUCTION

Separation of gases accounts for the major production costs in chemical, petrochemical, and related industries. There has been a growing demand for economical and energy-efficient gas separation processes. Although cryogenics and absorption remain the most widely used processes for this purpose, the last two decades have seen a tremendous growth in research activities and commercial applications of adsorption-based gas separation processes. The increasing interest in this area is also reflected in the large number of research articles and patents published in the field of adsorption separation (*1*). Such a growing relevance of this area can be attributed to the following factors:

Development of synthetic and more selective adsorbents.
An improved theoretical understanding of adsorption from gaseous mixtures.
A better understanding of multicomponent adsorber dynamics.
Development of an efficient pressure swing cycle.

There have been several excellent review articles in the literature on pressure swing adsorption as a gas separation technique (*2–15*). These are generally concerned with the process or the applications. In the present review, the recent status of pressure swing adsorption (PSA) as a gas separating process is described. We include such recent developments of adsorbents as zeolites, carbon molecular sieves, and the newly emerging pore-engineered molecular sieves as well as the present day understanding of adsorption from mixtures. The focus is on specific commercial applications rather than on a mere survey of the literature.

THE BASIC PRINCIPLE OF PSA

Separation by an adsorptive process is based on the selective accumulation of one or more components of a gas mixture on the surface of a microporous solid. When a gaseous mixture is exposed to an adsorbent for a sufficient time, an equilibrium is established between the adsorbed phase and the gas phase. The adsorbed phase often has a composition different from that of the bulk phase. The gas phase becomes richer in the less selectively adsorbed component, as depicted in Fig. 1. The attractive forces responsible for adsorption are of the van der Waals type. Desorption can be achieved either by increasing the temperature of the system or by reducing the adsorbate pressure. The desorption step also regenerates the adsorbent surface for reuse during the subsequent adsorption step. Thus, the adsorptive separation process consists of a cyclic sequence of adsorption

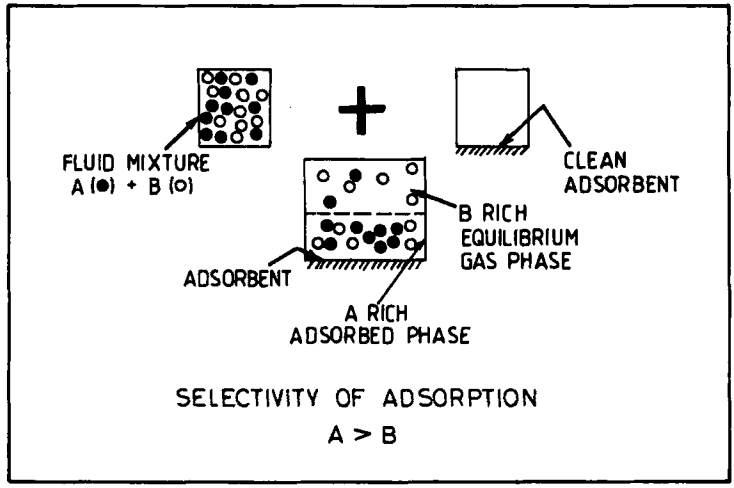

FIG. 1. Principle of adsorptive separation.

and desorption steps. When desorption is achieved by decreasing the pressure, the process is called pressure swing adsorption (PSA). One of the components is selectively adsorbed at higher partial pressure and desorbed subsequently by lowering the partial pressure. The change in the partial pressure of the component can be caused either by decreasing the total pressure, by changing the composition of the gaseous mixture, or by doing both simultaneously. Figure 2 shows the amount of gas adsorbed as a function of partial pressure at a particular temperature. The amount adsorbed decreases along the curve from Point A to Point B with a decrease in the partial pressure of the component. The adsorption capacity available for separation in PSA is the difference in the capacities for the given component at the two pressures. However, in practice, due to the heat of adsorption, there is an associated change in the temperature of the system and hence the working PSA capacity is slightly different, as depicted in Fig. 3.

THE PRIMARY STEPS IN PSA

The original PSA system was developed by Skarstrom (*2*, *16*, *17*) for air drying, which he called heatless drying. The PSA system in its basic form consists of two beds which are alternately pressurized and depressurized according to a programmed sequence. A two-bed system is shown

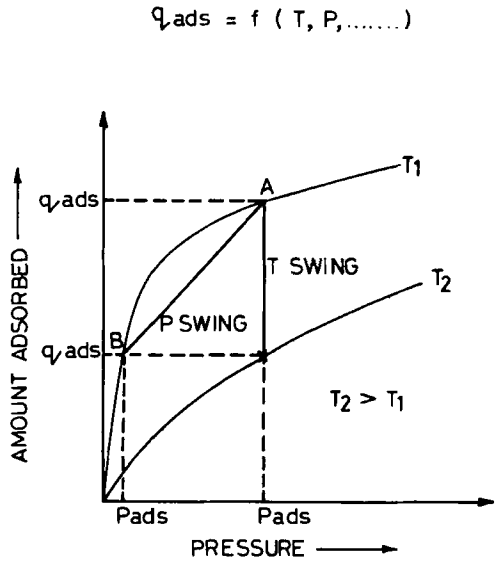

FIG. 2. Adsorption isotherms showing pressure and temperature swings.

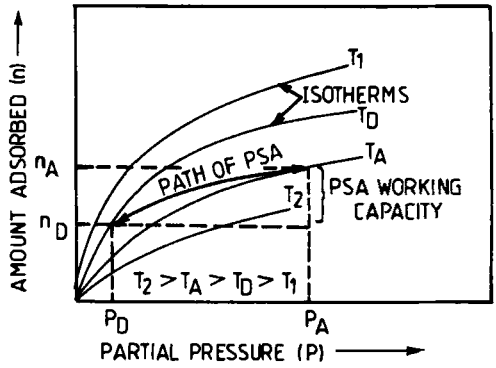

FIG. 3. Adsorption isotherms showing pressure and temperature swings and PSA working capacity.

in Fig. 4. The basic steps of the PSA process are shown in Fig. 5 and summarized in the following.

1. Feed Pressurization

The feed gas is compressed into an adsorbent-fixed bed from one end, with the other end being closed. The gas freed from the adsorbed components is accumulated at the closed end.

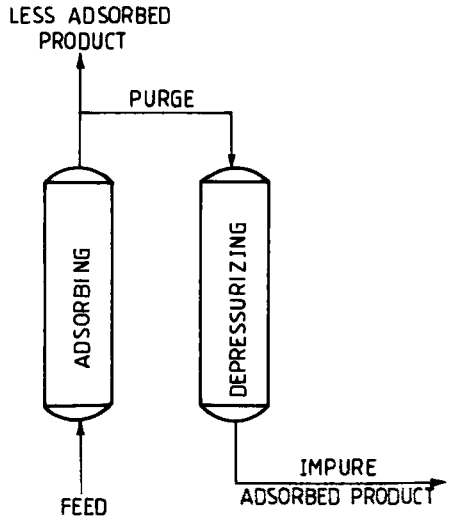

FIG. 4. Schematic diagram of a two-bed PSA process.

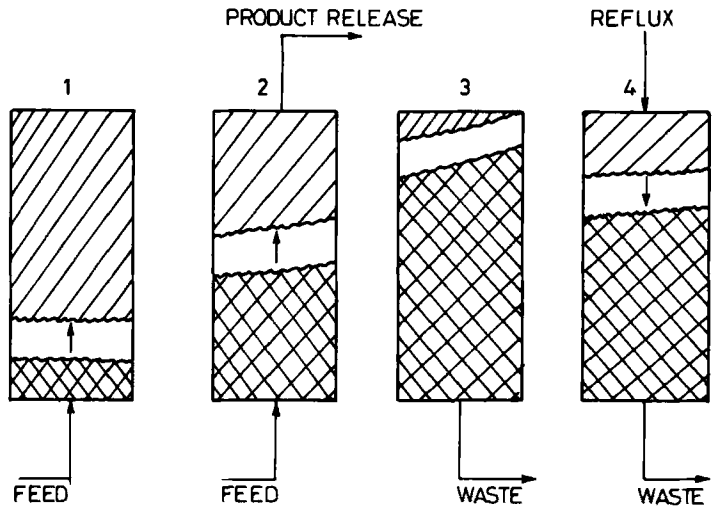

FIG. 5. The basic steps in a PSA process.

2. Product Release

At the upper operating pressure, the adsorbate-free gas, usually the product, is withdrawn from the far end of the bed while feed flow is maintained. Three distinct regions develop inside the adsorbent bed, as shown in Fig. 5.

(*a*) Near the feed entry the bed is saturated with the adsorbate and the gas phase has the composition of the feed.
(*b*) Near the exit the bed is still adsorbate free and the gas phase has the product composition.
(*c*) The region lying between the above two ends is called the mass transfer zone. This is where adsorption is occurring, and the gas phase composition changes rapidly along the axial position. The adsorption front moves along the bed as more feed is introduced. Eventually the bed is completely saturated, with the mass transfer zone having reached the end of the bed, at which point the feed is said to "breakthrough" into the product stream.

3. Depressurization

To regenerate the saturated bed, the next step involves reducing the operating pressure (blowdown or depressurization). The adsorbate is largely desorbed into the gas phase, released as a waste stream, or collected as a product in case it is valuable.

4. Low Pressure Purge

To complete the regeneration of the bed, the adsorbent is purged with product quality gas at low pressure, usually countercurrent to the feed flow from the product end. In this case also, distinct regions form and the purge gas will eventually breakthrough the waste.

PSA is well suited to rapid cycling, and it generally operates at a relatively low adsorbent loading because selectivity is greatest in the Henry's law region. A high pressure operation is desirable because it minimizes the purge loss, but this gain is offset by the greater blowdown losses for a high pressure system. A low temperature operation is needed to maximize capacity and selectivity, but cooling below the ambient temperature is generally not economical. Some of the points that make separation by PSA economically attractive are the following:

A high concentration of the desired and less strongly adsorbed component in the gas mixture.

Moderate purity requirement for the desorbed product.

A low heat of adsorption (less than 30 kJ/mol) of adsorbable component to facilitate rapid desorption.

A linear adsorption isotherm for the strongly adsorbed component.

Small adsorption/desorption pressure ration.

MAJOR DEVELOPMENTS IN THE PSA PROCESS

One of the major disadvantages of the earliest PSA system was low recovery of the product gas. For example, in the separation of air for oxygen production, the recovery was rarely above 25% in a simple two-bed system. To overcome this disadvantage, a variety of process modifications have been made (*5*, *13*). A critical review of the literature during the past two decades shows that the major part of research in this area has been directed toward improving the process economy by enhancing the product recovery. Some of the most important developments are briefly described in the following.

Pressure Equalization Step

The major operating cost in PSA is the energy required for pressurization of the feed. In the early PSA systems a large part of this energy was lost during blowdown. Berlin (*18*) suggested a pressure equalization step to conserve this energy. After the first bed has been purged and the second bed has completed the adsorption step, instead of blowing down the second bed directly, both the beds are interconnected to equalize the pressure. The first bed is partially pressurized with the product-rich gas from the

outlet of the second bed. Following pressure equalization, the beds are disconnected and the first bed is pressurized with the feed gas while the second bed is vented to complete blowdown. Inclusion of this step in the PSA process sequence has not only minimized energy losses but also resulted in a substantial increase in recovery.

Multibed System

More complex processes (*19*), including three- and four-bed systems, have been developed to take advantage of the pressure equalization step. A four-bed PSA system is shown in Fig. 6. In this system, one bed is in the adsorption step and the other three beds are in various stages of repressurization, depressurization, or purging. The principle is an extension of the Berlin system. The process operates at two intermediate pressures between the feed pressure and the exhaust pressure (usually atmospheric). At the end of the adsorption step, Bed 2, which is at high pressure, is connected at the discharge end to Column 4, which has just completed the purge step and is essentially at atmospheric pressure, and the pressures are equalized. In this way the product-rich gas is conserved and used for partial pressurization of Bed 4. Final repressurization of Bed 4 is accom-

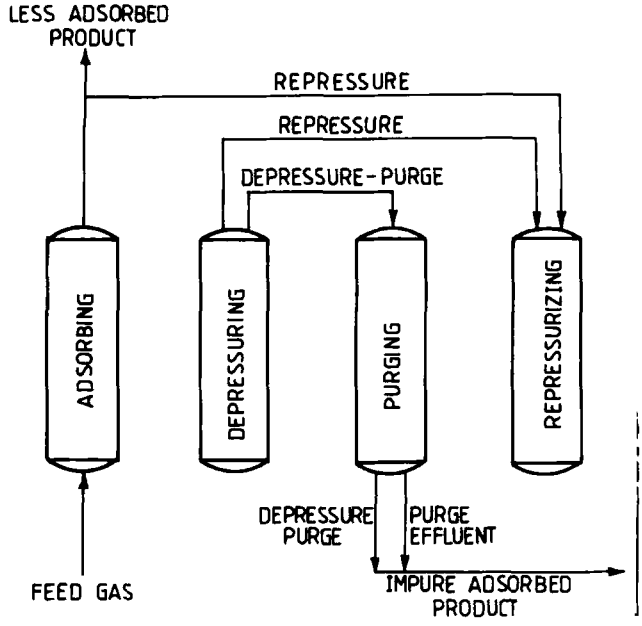

FIG. 6. Schematic diagram of a four-bed PSA process.

plished by using product gas from Bed 1, and then feed is connected to the inlet of Column 4. A fraction of the remaining gas from Bed 2 is used for reverse-flow purging of Bed 3. When the pressure in Bed 2 has fallen to the required level, Beds 2 and 3 are disconnected and the residual gas from Bed 2 is vented from the bed inlet. Bed 2 is then purged in reverse flow with gas from Bed 1 and repressurized to the first intermediate pressure with gas from Bed 4, which has just completed the adsorption step. The final repressurization is accomplished by using product gas, and the feed is then connected to the inlet of Bed 2. The advantages over the two-bed process at the cost of a more complex flow sheet are the following:

Considerable reduction in power consumption.
High product recovery
High purity product.
Constant product flow rate.

The use of more than one type of adsorbent in a single PSA unit, a guard bed to remove impurities, and rapid cycling to improve the adsorbent productivity are some of the other recent improvements (*13*). Other developments in the process include vacuum swing adsorption (VSA), polybed PSA (up to 10 beds), and multiproduct recovery. Recently, a process has been proposed (*20*) which can simultaneously produce an ammonia synthesis gas, a high purity CO_2, and a fuel gas containing small quantities of CO_2. This provides a perfect fit for urea manufacture application where CO_2 and NH_3 are reacted to form urea. This shows that the scope of PSA is only limited by the imagination and ingenuity of the human mind.

ADSORBENTS USED IN PSA

The choice of an adsorbent for PSA application is governed by its adsorption capacity and selectivity for the desired component. The selectivity or the separation factor of Component A over B is given by

$$\alpha_{A/B} = x_A y_B / y_A x_B \quad (1)$$

where x and y are the adsorbed and the gas-phase concentrations. Simulation studies reveal (*14*) that for the process to be economical, the minimum acceptable intrinsic separation factor for the desired component is about 3. With a separation factor of less than 2, it is difficult to design a satisfactory process. The benefits of an increase in the separation factor beyond 4 are insignificant. There are three factors used singly or in combination for achieving the desired selectivity:

Steric factors such as difference in the shape and the size of adsorbate molecules.

Equilibrium effect, i.e., when the adsorption isotherms of the components of the gas mixture differ appreciably.

Kinetic effect, when the components have substantially different adsorption rates.

Some of the adsorbents which have found or might find commercial PSA applications are described below.

Zeolite Molecular Sieves

The introduction of synthetic zeolites in the mid-1950s (*21–26*) made selective adsorption a major separation technology. Structurally, zeolite is a crystalline aluminosilicate with a framework based on an extensive three-dimensional network of AlO_4 and SiO_4 tetrahedra. The AlO_4 in the structure gives rise to an anionic charge in the framework. This is balanced by the cations that occupy nonframework positions. A general formula of the zeolites is

$$M_{n/2}O \cdot Al_2O_3 \cdot xSiO_2 \cdot yH_2O \qquad (2)$$

where M is the exchangeable cation and n is its valency. The value of x is equal to or greater than 2 because Al^{3+} does not occupy adjacent tetrahedral sites. Mainly alkaline and alkaline earth cations form the exchangeable cations. The structure of the crystal framework contains voids (cavities, pores) and channels of molecular dimensions. The pore or channel openings range from 3 to 10 Å, depending on the structure. Framework structures of zeolites A and X are shown in Fig. 7. Synthesis and characterization of zeolites have been dealt with in detail by Breck (*21*, *23*) and

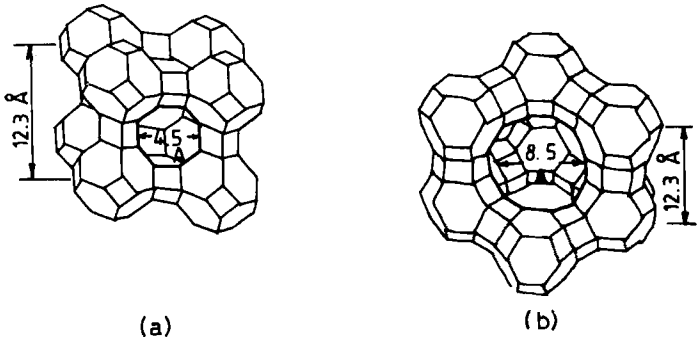

FIG. 7. Framework structures of (a) zeolite A and (b) zeolite X and Y.

recently by Szostak (*22*). Some of the unique features which make zeolites useful for separation processes are:

An unusually high thermal and hydrothermal stability.
A uniform pore structure.
Easy pore aperture modification.
High adsorption capacity even at low adsorbate pressure/concentration.
Substantial adsorption capacity at moderately elevated temperature.

Though more than 150 species of synthetic zeolites are known, only some of them have found commercial application as an adsorbent. The following factors largely dictate the choice of a zeolite for its commercial use:

High capacity/product yield.
High selectivity.
Chemical stability and economics.

Carbon Molecular Sieves

Carbon molecular sieves differ from activated carbon in pore size distribution as shown in Fig. 8. These have pores in a narrow range approximately between 5 and 10 Å and pore volume does not exceed a value of 0.25 cm^3/g, whereas activated carbon exhibits a considerably higher pore volume and average pore diameter up to 20 Å (*27*, *28*). Manufacturing

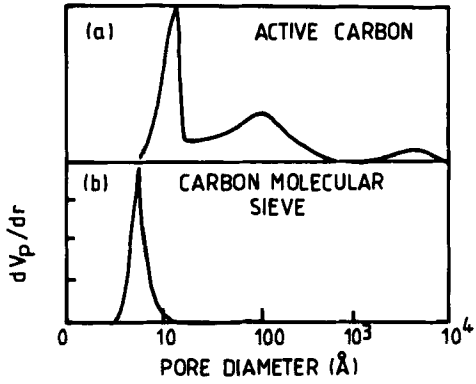

FIG. 8. Pore size distribution for (a) activated carbon (V_p = 0.95 cm^3/g) and (b) carbon molecular sieve (V_p = 0.25 cm^3/g).

methods for carbon molecular sieves are a guarded secret and involve techniques such as pyrolysis of polymers, thermal treatment of anthracite, and thermal treatment with subsequent cracking of hydrocarbons (*29–33*). The basic steps involved in the production of carbon molecular sieve are:

Carbonization of carbonaceous material in an inert atmosphere.
Pelletization of the carbonized material thus formed by using binders.
Controlled gasification of the pellets followed by carbon deposition on the pore mouths.

An overview of the work done in the preparation of carbon molecular sieves is given in Table 1 (*34*).

There are three companies producing commercial carbon molecular sieves: Bergbau-Forschang GmbH of West Germany, Takeda Chemical Company of Japan, and Calgon Corporation of USA. Bergbau-Forschang has the technical know-how for the manufacture of carbon molecular sieves, and their process is reported (*31*) to be broadly based on hard-coal oxidation in air as well as an additional method for controlling the pore structure, e.g., a cracking of hydrocarbons within the micropore system or a careful partial gasification. The raw material, bituminous coal, is ground to 90% passing 40 μm. This is then air oxidized in a fluidized bed to form oxicoal which is pelletized with a binder into granules. Shaped material is carbonized in a rotary drum to a uniformly formed material. This can be used to produce two different types of molecular sieves, one for hydrogen/helium purification and the other for nitrogen production from air. In the former the pores are enlarged by mild steam activation, whereas in the latter the pore mouths are partially blocked by cracking hydrocarbons so that they deposit a thin layer of coke at the pore mouths. Both types of pores are shown in Fig. 9. However, the lack of absolute reproducibility among different commercial batches always leads to a very narrow distribution of pore size. As a result, carbon molecular sieve selectivity is always inferior to the one achieved in zeolite molecular sieves.

Potential Adsorbents

Although there is some room for improvement in the PSA process, the potential gains in process economics in the future are likely to come from the development of new and improved adsorbents. Major advances have been made in the synthesis of new zeolite structures since the development of the first synthetic zeolite A. The development of silicalite (*58*), ZSM type (*59*), metallosilicates, aluminophosphates ALPOs (*60*), silicoaluminophosphates SAPOs (*61*), metalloaluminophosphates MeAPOs (*62*),

TABLE 1
An Overview of Work Done in the Preparation of Carbon Molecular Sieves

Raw material	Process and parameters	Adsorbate studied	Ref.
Sugar	Carbonization at 1000°C	*n*-Carboxylic acid, benzene, *n*-heptane	35
Anthracite	Carbonization followed by activation with CO_2 + CO at 1 atm	*n*-Butane, isobutane, and neopentane	36
Saran	Carbonization at 900°C (6–7°C/min) for 4 h; binding and pelletization with coal tar pitch, lignite pitch, or methyl cellulose followed by carbonization at 900°C (5°C/min) in an N_2 atm for 2 h. Optional activation at 800–850°C		37
Saran	Carbonization up to 1000°C (7.5°C/min) or up to 1500°C (15–30°C/min). Kept at 1500°C for 4 h	*n*-Butane, isobutane, and neopentane	38
High rank coal	Carbonization at 600–900°C followed by steam activation at 950°C		32
Wood (lauan chips)	Carbonization at 400–1000°C for 25 min; binding with coal tar pitch and water; drying at 100°C for 3 h; carbonization at 600–1000°C in an N_2 atmosphere		39
Mineral coal	Oxidation in air followed by binding and pelletization with soft pitch and water; heated to 800°C (10°C/min) followed by benzene cracking in N_2 at 800°C for 20 min	Separation of N_2/O_2, He/CH_4, and Ar/O_2	40
Peat	Binding with PhOH-HCHO followed by carbonization at 500–700°C and steam activation at 900°C		41
Coconut shell	Binding with 5 to 15% pitch, heat treatment in air flow at 300 to 400°C for 2–3 h, calcination at 850–900°C for 5–20 min		42
Anthracite	Oxidation in O_2 followed by carbonization at 1000°C		43
American noncoking and coking coals	Carbonization at 800–900°C (5°C/min) for 2 h preoxidation at 150–250°C	N_2/O_2 separation	44
Polyfurfuryl alcohol	Carbonization at 850°C for 1 h, steam activation at 850°C		45
CMS V	Heat treatment in N_2 stream at 145°C for 15 min; 305°C for 20 min; 527°C for 35 min; 665°C for 40 min. Carbon deposition with C_6H_6 (0.4–0.8 g/min) in an N_2 stream at 1000°C for 40 min	N_2O_2 mixture	46

Pine wood charcoal	Carbonization at 900°C for 20 min; at 800°C (5°/min) for 6 h in an Ar atmosphere	O_2 in air	*47*
Akahira coking coal	Binding with 12% molasses; carbonization; activation at 650–800°C	CO_2, *n*-butane, isobutane, and neopentane	*48*
Polyfurfuryl alcohol, polyvinylidene chloride urea formaldehyde, and Saran	Preparation of char; carbonization at 400–900°C in vacuum for 6 h; 180°C for 2 h; 600° for 12 h	N_2 and CO_2	*49*
Bituminous coal	Oxidation below ignition; binding; carbonization; steam activation/hydrocarbon treatment	N_2 and O_2	*31*
Saran	Carbonization at 600–900°C (2.5–20°C/min); binding with coal tar pitch (23.1%) and microcrystalline cellulose (7.5%)	*n*-Butane, isobutane, C_6H_6, and cyclohexane	*50*
Akahira char	Binding with sulfite pulp waste liquor; pelletization; carbonization at 200–1000°C (10°C/min) for 1 h		*51*
Polyvinyl alcohol	Carbonization at 400–1000°C for 3 h		*52*
High volatile bituminous	Granulation; carbonization at 650–950°C and 25 MPa		*53*
Noncoking coal	Carbonization at 550–800°C for 2 h; binding with starch paste/aqueous phenolic resin (20–30%); pelletization; drying (110°C, 2 h); carbonization (160°C, 4 h)	CO_2, benzene, and isobutane	*54*
Coconut shell char	Heat treatment at >482°C (5°C/min) in O_2-free atmosphere		*55*
Coal	Carbonization at 850°C for 30 min; activation in CO_2 atmosphere at 850°C for 4 h; binding with 5 wt% coal tar and naphthalene oil; carbonization at 900°C for 20 min	N_2 from air	*56*
Semicake (≤5% volatiles)	Heat treatment in inert gas + steam (20–95 vol%) at 800–900°C for 5–30 min; in inert gas with 5–12 vol% benzene at 750–800°C	O_2 from air	*57*

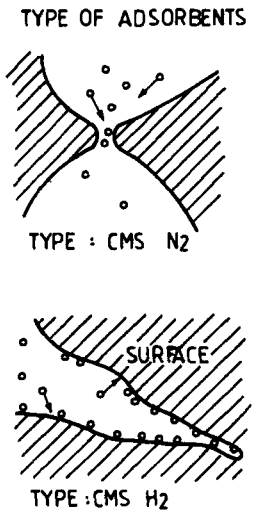

FIG. 9. Two types of pore structures in a carbon molecular sieve.

particularly the more recent synthesis of VPI-5 (*63*), aluminoborates (*64*), and beryllophosphates (*65*) shows that the field of zeolite synthesis is yet to reach its maturity even after the considerable synthetic efforts of the last 40 years. At present, mainly A, X, mordenite, and some natural zeolites are being commercially used as adsorbents in the separation of gases by PSA. The commercial potentials of such zeolites as silicalite, ZSM type, and ALPOs are yet to be explored. These present interesting and varied surfaces, and they call for extensive studies from the adsorption point of view. For example, silicalite has a highly hydrophobic surface, while A and X are strongly hydrophilic in nature. ALPOs, on the other hand, have an intermediate hydrophilicity. This class of zeolites may become specialized adsorbents for separation processes. Recent studies (*66*, *67*) have shown that silicalite is a potential adsorbent for the separation of N_2/CH_4 and CO_2/CH_4, with selectivities for N_2 and CO_2 being more than 3, as shown in Table 2.

Modification of the pore apertures of zeolites was largely confined to the exchanging cations until recently. Recent studies (*68–76*) have shown that the zeolite pores can be engineered to suit desired applications by additional techniques, viz.:

Preadsorption of polar molecules.

Internal or external surface modification by chemical reactions.

External surface modification of the zeolite crystal by chemical vapor deposition or other coating processes.

TABLE 2
Separation Factors for Sorption of CO_2, N_2, and CH_4 on silicalite

Temperature (K)	Separation factor		
	CO_2	CO_2/CH_4	CH_4/N_2
273	20	3.5	3.5
283		3.0	2.8
298		2.7	2.7
323		2.5	2.2
343	4	2.0	—

It has been observed (*75*, *76*) by us that if a small amount of polar molecules such as water, ammonia, or pyridine are preadsorbed on the internal or the external surface of a zeolite, the sorption of another adsorbate is affected substantially as seen in Fig. 10. The strong interactions between the zeolite cations and the polar molecules produce a diffusion block. Such a control of adsorption phenomenon, though not commercially utilized so far, appears to be a possibility, particularly for the separation of gases.

Vansant and coworkers (*68*) showed that treatment of zeolites with silane and diborane can be used to control the pore size of a zeolite (Figs. 11 and 12). However, an interesting possibility (*68*, *72*, *74*) of modification of zeolite pores for gas separations without affecting the internal cage structure is by chemically depositing the large molecules on the exterior of the zeolite. Silicon derivatives like $Si(OCH_3)_4$ and methyl chlorosilanes can be reacted with the hydroxyl groups on the external surface of the zeolite crystal followed by calcination in the presence of air, which leaves a silica-coated zeolite. The deposit of SiO_2 on the external surface results in modification of the pore size. The effect of the amount of silica deposition on *p*-xylene adsorption in H-mordenite was reported by Vansant (*68*). Niwa et al. (*74*) prepared an oxygen-selective zeolite A by chemical vapor deposition of silicon methoxide on zeolite A. The pore opening is narrowed down by the silica deposits and excludes the larger nitrogen molecules.

THEORIES OF MIXED GAS ADSORPTION

In a commercial adsorptive gas separation process, knowledge of mixed gas adsorption is very important for modeling and predicting the dynamics of an adsorbent bed. The experimental measurement of gaseous mixture adsorption is tedious and time consuming. A number of theoretical models have been proposed (*13*, *14*) to predict mixture adsorption from pure

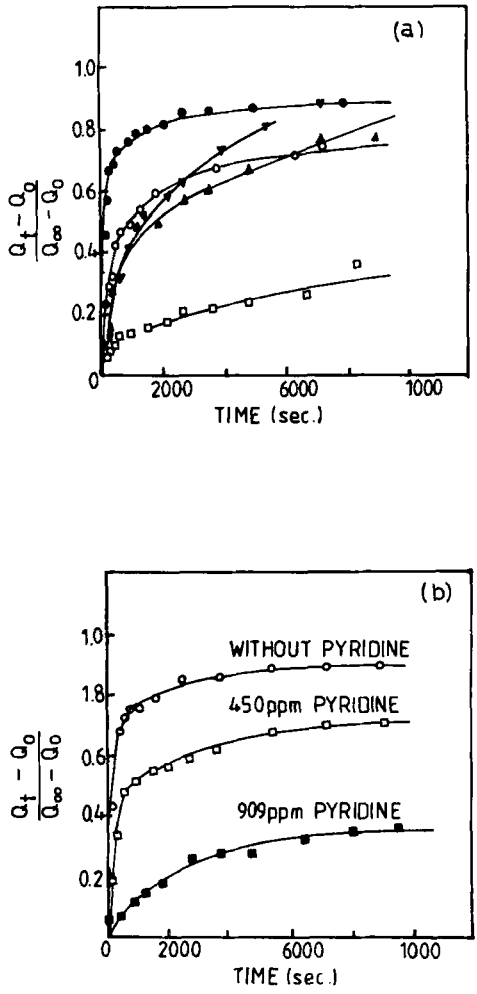

FIG. 10. Sorption uptake curves for *n*-dodecane from 1,3,5-trimethyl benzene on molecular sieve 5A having presorbed (a) △ water, ▲ cyclpentanol, ○ methanol, □ *t*-butyl alcohol, ● without presorbed component; (b) pyridine.

component adsorption data in the last two decades. A majority of these models predict the mixture behavior only for a limited number of cases. The lack of accurate knowledge of mixture adsorption under process conditions remains the weakest link in a PSA process. We describe here some of the models which have been used with a fair degree of success.

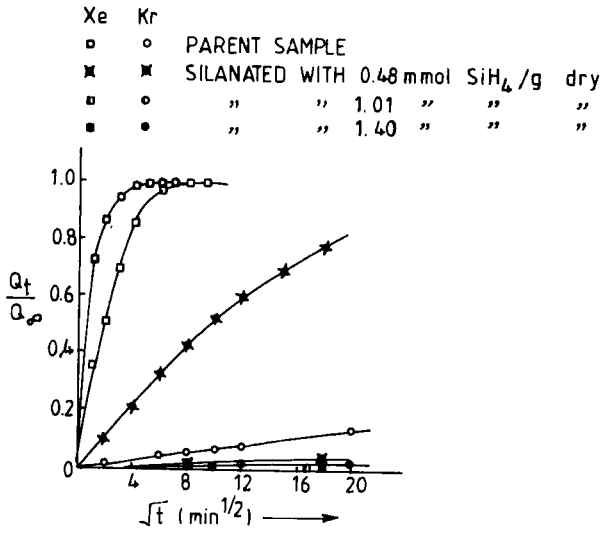

FIG. 11. Influence of silanation on the sorption of krypton and xenon at 273 K on mordenite.

Extended Langmuir Theory

Markham and Benton (*77*) extended the Langmuir equation for the pure component to a mixture of n components as

$$\theta_i = b_i p_i \Big/ \left(1 + \sum_{j=1} b_j p_j\right) \tag{3}$$

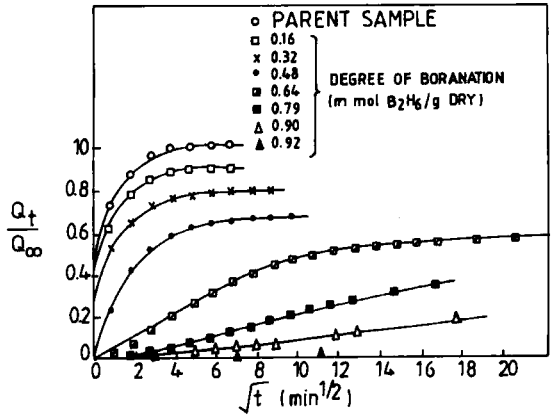

FIG. 12. Influence of boranation on the sorption of xenon at 273 K on mordenite.

where b_i is the Langmuir constant, p_i is the partial pressure, and θ_i is the fraction of coverage for component i. It has been shown (*78*, *79*) that this model is thermodynamically unsound. Despite its lack of a rigorous thermodynamic basis and the inbuilt weaknesses of the Langmuir model itself, the Extended Langmuir equation is widely used for modeling the adsorber dynamics, largely because of its mathematical simplicity. Bhat et al. (*80*, *81*) further simplified the Extended Langmuir equation for predictions of adsorption phase diagrams. It has been tested for adsorbents such as silica gel, activated carbon, zeolites 5A and 13X, carbon molecular sieve, etc.

Yon and Turnock (*82*) proposed a combined Langmuir–Freundlich equation for mixtures with the concept of monolayer capacity replaced by maximum attainable capacity for zeolites. For a binary mixture, the equation is

$$\theta_i = b_i p_i^{1/n_i} \Big/ \left[1 + \sum_{j=1} b_j p_j^{1/n_j}\right] \tag{4}$$

The term θ_i is called the loading ratio, and the above equations are also described as loading ratio correlations.

Ideal Adsorbed Solution Theory (IAST)

IAST, given by Myers and Prausnitz (*83*), treats the mixed adsorbed phase as a solution in equilibrium with the gas phase. The fundamental thermodynamic relations for liquids are then applied to the adsorbed phase. The assumptions of an ideal adsorbed phase, thermodynamically inert adsorbent, and temperature invariant adsorbent area are made. To use the thermodynamic equations for the two-dimensional adsorbed phase, the spreading pressure is substituted for pressure and the area for volume. The equilibrium between an ideal gas and the adsorbed phase is expressed as

$$py_i = x_i p_i^\circ(\Pi) \tag{5}$$

where p_i° for vapor–liquid equilibrium is the vapor pressure of the pure saturated liquid at the temperature of the solution. In this case, $p_i^\circ(\Pi)$ is the equilibrium pressure in the gas phase corresponding to the solution spreading pressure for adsorption of pure component i. The spreading pressures of the adsorbates are equal at adsorption equilibrium. The relation between the spreading pressure and the pressure of the pure component is obtained by integration of the Gibbs adsorption isotherm

$$\Pi_i^\circ A/RT = \int_0^{p_i} v_i^\circ dp/p \tag{6}$$

Thus, the spreading pressure can be determined from the pure component adsorption isotherm by using this equation.

For a binary mixture, the following equations can be written:

$$\Pi_1^\circ A/RT = \int_0^{p_1^\circ} v_1^\circ dp/p; \qquad \Pi_2^\circ A/RT = \int_0^{p_2^\circ} v_2^\circ dp/p \tag{7}$$

$$Py_1 = p_1^\circ x_1; \qquad Py_2 = p_2^\circ x_2 \tag{8}$$

$$\Pi_1^\circ = \Pi_2^\circ = \Pi \tag{9}$$

$$x_1 + x_2 = 1; \qquad y_1 + y_2 = 1 \tag{10}$$

If we specify two variables like P and y_i, the other variables can be calculated by using these equations. For an ideal adsorbed solution, the changes in area and enthalpy for a hypothetical mixing are zero, which lead to

$$a_{\text{mix}} = a_1^\circ(\Pi)\, x_1 + a_2^\circ(\Pi)\, x_2 \tag{11}$$

where a_i° is the area occupied per mole of the component i. This is proportional to $1/V_i$. Thus the relation to calculate mixture adsorption becomes

$$1/V_{\text{mix}} = x_1/V_1^\circ(\Pi) + x_2/V_2^\circ(\Pi) \tag{12}$$

IAST is the most widely tested theory for mixtures, including binary and ternary mixtures on silica gel, activated carbon, and zeolites (*13*, *14*, *84*, *85*). Many systems have shown deviation from the predicted data. Attempts have been made to account for deviations by using activity coefficients for mixed adsorbed species (*13*, *86*). IAST does not need a specific isotherm for the description of pure component data. But the main disadvantage lies in having to extend the pure component data too far above the total binary pressure in order to obtain appropriate pressure–spreading pressure data for individual components.

Vacancy Solution Theory (VST)

Vacancy solution theory, developed by Suwanayuen and Danner (*87*) for pure gases as well as mixtures, is based on the following concepts:

Both the gas and adsorbed phase are considered to be the solutions of adsorbate in a hypothetical solvent called vacancy. A vacancy is a

vacuum entity occupying a space that can be filled by an adsorbate molecule.

Properties of an adsorbed phase are defined as excess properties in relation to a dividing surface.

The entire system, including the solid, is in thermal equilibrium, but only gas and the adsorbed solution are in osmotic equilibrium with each other.

Equilibrium of the system is maintained by spreading pressure which arises from a potential force field at the surface.

The isotherm equation for a pure component is given as follows:

$$p = \left[\frac{n_1^{s,\infty}}{b_1}\frac{\theta}{1-\theta}\right]\left[\Lambda_{iv}\frac{1-(1-\Lambda_{vi})\theta}{\Lambda_{iv}+(1-\Lambda_{iv})\theta}\right] \times \exp\left[-\frac{\Lambda_{vi}(1-\Lambda_{iv})\theta}{1-(1-\Lambda_{vi})\theta} - \frac{(1-\Lambda_{iv})\theta}{\Lambda_{iv}+(1-\Lambda_{iv})\theta}\right] \quad (13)$$

where p is the equilibrium pressure, θ is the coverage, and $n_i^{s,\infty}$ is the saturation capacity. This equation has four parameters: b_1, $n_1^{s,\infty}$, Λ_{iv}, and Λ_{vi}. The parameters Λ_{iv} and Λ_{vi} account for the adsorbate–adsorbent interactions.

A similar concept has been used (*87*) to develop a model to predict mixture adsorption. In a binary mixture the equilibrium is between two ternary vacancy solutions. Equating the chemical potentials for the adsorbed and the gas phase, and using the Luscassen–Reyenders (*87*) expression for chemical potential of the adsorbed phase, the following equation results if the gas is assumed to be ideal:

$$Py_i = \gamma_i^s x_i \frac{n_m^s}{n_m^{s,\infty}} \exp(\Delta G_i^\circ/RT) \exp(\Pi a_i/RT) \quad (14)$$

This is the basic equation to be solved in VST for predicting the mixture adsorption. This equation relates the gas-phase mole fraction of component y_i with the adsorbed phase mole fraction x_i.

The expressions used for the spreading pressure and the free energy are

$$-\Pi a_i/RT = \left[1 + \frac{n_m^{s,\infty} - n_i^{s,\infty}}{n_m^s}\right] \ln \gamma_v^s x_v^s \quad (15)$$

$$\exp(\Delta G_i^\circ/RT) = (y_i P/\gamma_i^s x_i^s) \exp(-\Pi a_i/RT) \quad (16)$$

where γ_i^s is the activity coefficient of adsorbed component i. In the first paper on VST, Wilson's equation was used for the activity coefficient:

$$\ln \gamma_k = 1 - \ln \left[\sum_{j=1}^{n} x_j \Lambda_{kj} \right] - \sum_{i=1}^{n} \left[\frac{x \Lambda_{ik}}{\sum_{j=1}^{n} x_j \Lambda_{ij}} \right] \tag{17}$$

which leads to the final equation

$$Py_i = (\gamma_i^s x_i n_m^s n_i^{s,\infty} \Lambda_{iv} / n_m^{s,\infty} b_i) \exp (\Lambda_{vi} - 1) \exp (\Pi a_i / RT) \tag{18}$$

All the parameters in this model except Λ_{12} and Λ_{21} are obtained from the pure component isotherm regression which can be used to determine the mixture adsorption. Suwanayuen and Danner (*87*) suggested a method for estimating Λ_{12} and Λ_{21} from pure component data. VST has been shown (*13*, *84*) to predict the mixture adsorption on zeolites and activated carbon. Hyun and Danner (*88*) showed that VST can also predict the adsorption azeotropy observed in some cases.

Cochran and Danner (*89*) modified the above model using Flory–Huggins activity coefficients. This leads to a reduction of one parameter in the isotherm, thus making the regression easier without any loss of accuracy.

Simplified Statistical Thermodynamic Theory (SSTT)

Ruthven et al. (*14*, *90*) proposed a statistical thermodynamic model which includes lateral interactions between sorbed species by using the following basic assumptions:

The sorbate–sorbent interactions are independent of sorbate concentration and can be represented by the Henry's law constant, k.

The sorbate–sorbate interactions are represented by the reduction in the free volume of the zeolitic cavities, V.

The sorbed molecules are confined within particular cavities of the zeolite lattice but are not sorbed at specific sites within the cavities.

The pure component isotherm is given by the equation

$$C = \frac{kp + (kp)^2(1 - 2\beta/V)^2 + \cdots + [(kp)^m/(m-1)!](1 - m\beta/V)^m}{1 + kp + 1/2(kp)^2(1 - 2\beta/V)^2 + \cdots + [(kp)^m/m!](1 - m\beta)/V)m} \tag{19}$$

where m is the number of molecules of sorbate and β is the molecular volume of the sorbate. The corresponding expression for binary mixture

sorption of Components A and B is given as

$$C_A = \frac{k_A p_A + \sum_j [(k_A p_A)^i (k_B p_B)^j (1 - i\beta_A/V - j\beta_B/v)^{i-j}/(i-1)!j!]}{1 + k_A p_A + k_B p_B + \sum_j \sum_i (k_A p_A)^i (k_B p_B)^j (1 - i\beta_A/v - j\beta_B/v)^{i+j}/i!j!} \quad (20)$$

where i and u are the number of molecules of A and B, respectively, in a particular cage, and β_A and β_B are the molecular volumes of A and B. Summations in the above equation are evaluated over all values of the indices i and j satisfying the condition $i + j \geq 2$ and $ib + jb \leq v$. Henry constants can be determined from the pure component isotherms. Molecular volumes are estimated by the van der Waals covolume. Equation (20) can then be directly used to predict the mixture adsorption isotherm. This theroy has been tested for C_2 to C_4 hydrocarbons and CO_2 on zeolite 5A (*14*). Fielder et al. (*91*) used this theory for the adsorption of krypton and xenon on 5A, and heptane and xylene on 13X. However, this equation appears to be best suited for large nonpolar molecules of similar size.

A comparison (*14*, *84*) of various theories for mixture adsorption shows that no single model is capable of predicting the adsorption equilibria for all types of mixtures under different conditions of temperature and pressure. Further, the available data base on mixture adsorption is too limited to rigorously test the validity of the various models. However, some general comments about these models can be made:

SSTT is the most satisfactory model for the adsorption of large molecules of similar sizes in zeolites.

VST has not been extensively tested but has been found satisfactory for zeolites.

IAST is the most widely tested theory but is of limited applicability for adsorption on zeolites.

The extended Langmuir and Langmuir–Freundlich models remain the most widely used ones in commercial applications.

The design and operation of an adsorber bed requires the knowledge/estimation of cycle time, breakthrough curve, adsorption capacity, product recovery and purity, etc. These are estimated by using theoretical models. Major developments have taken place on this front during the last two decades. The three models for PSA which are fairly described in the literature (*13*, *14*) are the following:

(*a*) The *equilibrium model* assumes that the gas contacting the bed is in equilibrium with the adsorbent particle. As the gas composition

changes with time, the rate of adsorption, dc_{sci}/dt, is calculated, where dc_{sci} is the equilibrium surface concentration of component i. This assumption is useful for the preliminary analysis of PSA.

(*b*) The *diffusion model* is based on the observation that under most adsorption process conditions, the surface adsorption rate is very high compared with the mass transfer process occurring in the adsorbent, and hence the rate-determining step is the diffusion through the adsorbed pores.

(*c*) The *linear driving force model* is an approximation to the solution of the Fick's diffusion equation for a spherical particle. This expression assumes that the adsorption rate is proportional to the equilibrium concentration of the component in the gas phase minus the actual concentration of the component in the adsorbed phase.

To obtain the mass balance between the feed mixture and the adsorption system with respect to each component or for an overall mass balance, experimental mixture adsorption isotherm data or the data predicted from pure component isotherms by using the theoretical models previously described are employed. It has been observed from the literature that Extended Langmuir or Langmuir–Freundlich isotherms for mixture adsorption are the most widely used models for this purpose. Models such as IAST, VST, and SSTT are not preferred because of their mathematical complexity.

APPLICATIONS OF PRESSURE SWING ADSORPTION

The earliest applications of PSA were in the area of drying and purifications of gases by selectively removing the strongly adsorbing impurities from gas streams. However, of late, it is finding greater application for the bulk separation of gases. Some of the commercially used PSA processes for the separations of gases are described below.

Air Separation

PSA units are widely used for the separation of air as an alternative to the conventional cryogenic separation process. Two different processes are in use. The zeolite molecular sieve-based process, largely used for oxygen production, utilizes zeolite adsorbents which show preferential adsorption toward nitrogen under equilibrium conditions. The carbon molecular sieve-based process, used for nitrogen production, depends on a kinetic separation achieved by a faster diffusion of oxygen molecules.

Oxygen Production

The different zeolites used for this application include NaA, CaA, NaX, CaX and other cation-exchanged X, CaY, mordenite, chabazite, erionite,

etc. Separation is achieved as a result of the difference in the adsorption affinities of nitrogen and oxygen. Nitrogen molecules possessing a quadrupole moment of 0.31 A^3 interact more strongly with the cations of zeolites than oxygen molecules with a quadrupole moment of 0.1 A^3. The experimental equilibrium data (*92*) for nitrogen, oxygen, and argon on 5A are shown in Fig. 13. Because argon is adsorbed to the same extent as oxygen, as shown in Fig. 13, the maximum oxygen purity achieved is 95–96%. An adsorbent for oxygen production should have a higher nitrogen adsorption capacity and selectivity. The following are the major factors that affect the nitrogen capacity and selectivity of a given zeolite molecular sieve.

Nature of the Cation

In general, in a given zeolite the interaction energy and thus the capacity for nitrogen increases with the charge density of the cation (*20*, *93*, *94*). As seen in Table 3, for monovalent alkali metal exchanged X zeolites, nitrogen adsorption capacity shows the following trend: $Li^+ > Na^+ > K^+ > Rb^+ > Cs^+$.

N_2/O_2 selectivity follows the same trend as the nitrogen capacity. A correlation of cation–quadrupole interaction energies, ϕ_{F-Q}, with the selectivity for nitrogen by univalent ion exchanged zeolite X is shown in Fig. 14. Oxygen, with its smaller cation–quadrupole interaction energy, is much less sensitive to the cation present. Similar trends may be expected with the polyvalent cations due to their high charge density. However, they are often more sensitive to the activation procedure, which is explained in succeeding sections.

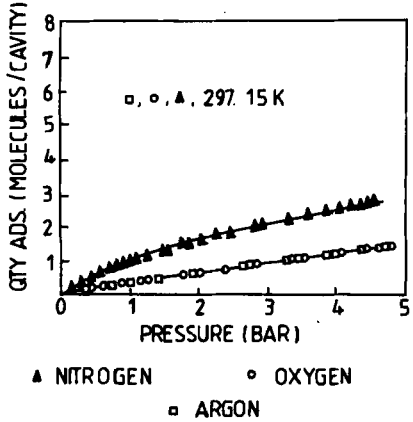

FIG. 13. Pure component equilibrium adsorption data of N_2, O_2, and Ar on molecular sieve 5A at 297.15 K.

TABLE 3
Selectivity and Capacity of Ion-Exchanged X Zeolites at −78°C for a 25% O_2–75% N_2 Mixture at 1 atm Total Pressure

Adsorbent	Ion-exchange level	N_2/O_2	Adsorption capacity for N_2 (cm^3 STP/g)
LiX	86	7.6	111.8
NaX	100	4.9	72.4
KX	100	2.2	58.7
RbX	56	3.5	30.0
CsX	50	1.3	26.3

Extent of Cation Exchange

In general, nitrogen capacity and selectivity increase with an increase in bivalent ion exchange. In the case of zeolite A, we have observed (*95*) an increase in nitrogen selectivity and capacity with an increase in calcium ion exchange, as shown in Fig. 15. It is claimed in the patent literature (*96*) that when zeolite A is exchanged by calcium ions to a level such that the zeolite has a Ca/Na_2O mole ratio exceeding 38.7 (weight ratio of 25), the adsorption capacity for nitrogen increases at a steep rate with increasing calcium exchange, with only a marginal increase in oxygen capacity. Figure

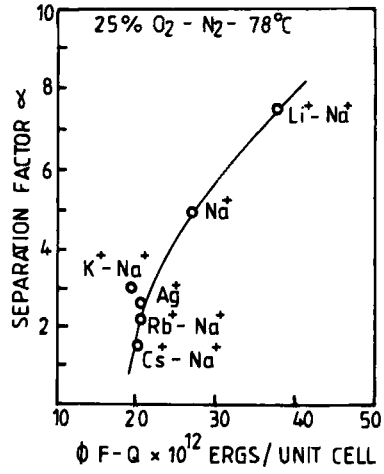

FIG. 14. Correlation of cation quadrupole energies (ϕ_{F-Q}) with the selectivity of nitrogen in a zeolite X.

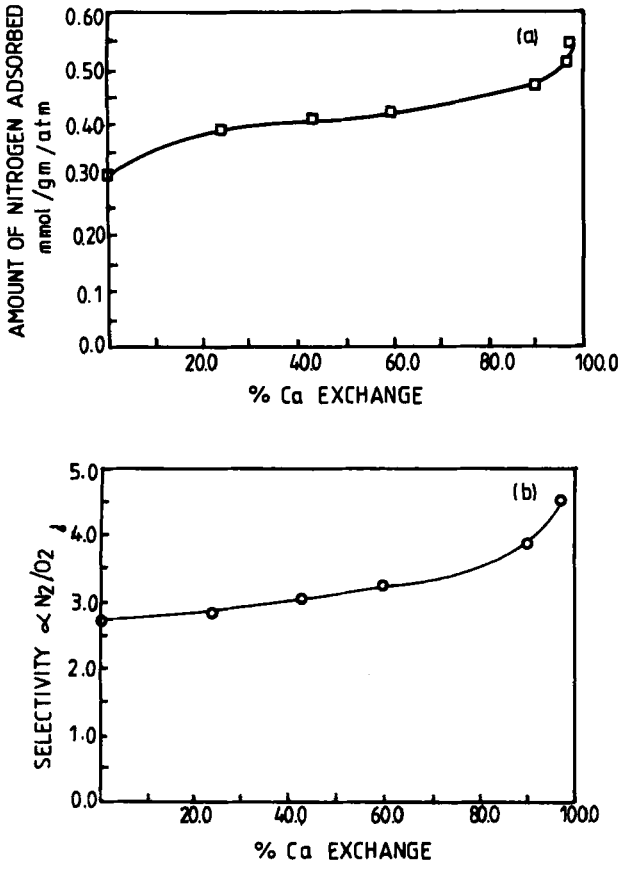

FIG. 15. Effect of calcium exchange in zeolite A on (a) N_2 adsorption capacity and (b) N_2/O_2 selectivity.

16 shows the adsorption capacities of nitrogen and oxygen on zeolite A as a function of the Ca/Na_2O weight ratio.

In the case of faujasite, the effect of calcium exchange on nitrogen adsorption capacity and selectivity is more pronounced than in A zeolite. Coe et al. (*97*) reported a fivefold increase in nitrogen selectivity on X zeolite when the calcium exchange was varied from 0 to 95% (Fig. 17).

Si/Al Ratio

The strength of the cation/sorbate interaction is relatively independent of the number of cations present (*98*). Hence the adsorption capacity for weakly interacting adsorbates such as nitrogen should be directly related to the number of sorbate-accessible cations in a zeolite. Therefore, if the

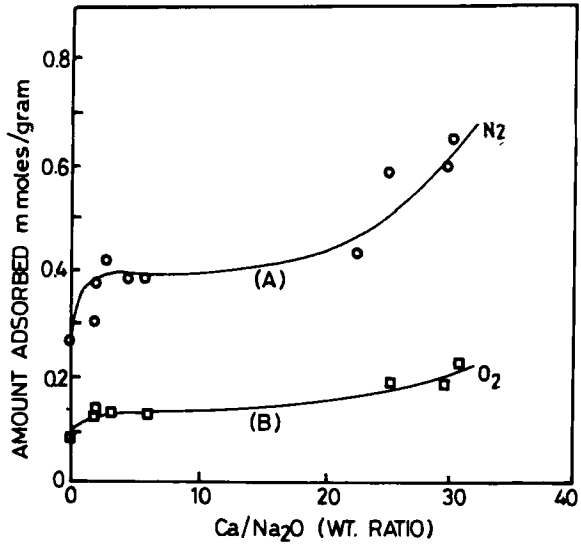

FIG. 16. Adsorption capacity for N_2 and O_2 on zeolite A as a function of increasing Ca/Na_2O weight ratio.

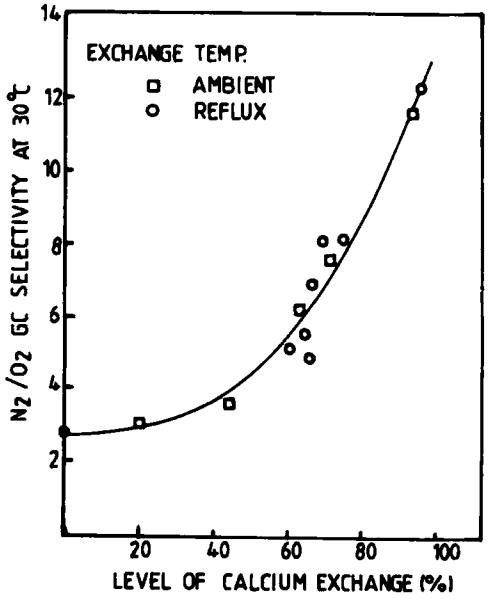

FIG. 17. Effect of calcium exchange in zeolite X on the selectivity of N_2.

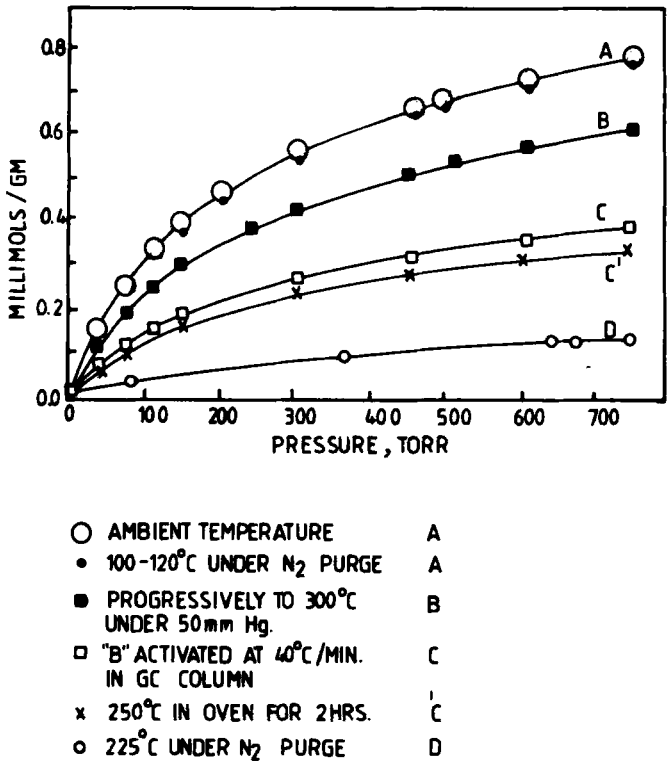

FIG. 18. Nitrogen adsorption isotherms at 303 K on CaX activated by various methods.

number of cations can be increased in a given zeolite, the nitrogen adsorption capacity can be increased. The number of cations in a zeolite depends on its Si/Al ratio. Coe et al. (*99*) reported a low silica X (LSX) with an Si/Al ratio equal to 1 (the typical value is 1.25). CaLSX contains about 18.5% more accessible cations than CaX which has an Si/Al of 1.25. This results into a 20% increase in nitrogen adsorption capacity. It is claimed that LSX possesses air separation properties superior to any other pelletized nitrogen selective adsorbent.

Activation of the Adsorbent

In any application of zeolites for adsorption purposes, the first step is to activate/regenerate the adsorbent in order to drive off the residual water. This is generally done by heating at high temperature. Recently Coe et al.

(*97*) reported a remarkable influence of activation procedure on the adsorption behavior of Ca-exchanged X zeolites. They concluded that in the case of polyvalent cation-exchanged zeolites, if thermal activation is not carried out properly (*97*), zeolites may undergo a substantial degree of hydroxylation. Figure 18 shows the effect of activation procedure on the adsorption capacity of nitrogen on CaX zeolite. Hydration is an equilibrium reaction represented as

$$M^{2+} + xH_2O \rightleftharpoons M(OH)^{(n-e)} + eH^+ + (x - e)H_2O$$

where M is a cation having valency n (usually 2 or 3), x is 1 to 6, and e is 1 or 2. Products on the right-hand side of the equation are detrimental to the zeolite capacity and stability. Hydroxylated multivalent cations, such as $Ca(OH)^+$, are known to be ineffective sites for selective adsorption, especially for nitrogen. Additionally, the zeolite framework is unstable toward H^+. The above equilibrium may be shifted toward the left by minimizing the amount of water present at any given temperature, particularly above 150°C, during activation. We recently observed (*69*) that even in zeolite 5A the initial activation procedure has a significant effect on the adsorption capacity and selectivity for nitrogen. It was found that zeolite 5A activated at 400°C for 12 h at a rate of 2°C/min under an inert gas purge gave about 16% higher nitrogen selectivity compared to a sample which was activated to 400°C for 12 h in an air oven at 30°C/min. A similar increase in the nitrogen adsorption capacity was also observed.

Mixture adsorption from binary as well as ternary mixtures of nitrogen, oxygen, and argon on 5A and 13X has been studied by various workers (*92*, *100–104*). These data can be used for process design and development.

Conventional PSA units for oxygen production contain a separate guard bed to remove such impurities as moisture and carbon dioxide from the feed air. Some units also employ a part of the adsorber beds as the guard bed for this purpose. The major applications of PSA oxygen include:

Biological treatment of industrial and municipal wastewater.
Feed to ozone generators for wastewater treatment.
Oxygen for rivers and reservoirs, especially for fish farming.
Bleaching of chemical pulp and treatment of black liquor in the paper industry.
Nonferrous smelting.
Welding applications.
Medical applications.

Chemical oxidation process.
Enriched oxygen combustion atmospheres to enhance fuel economy.

For the last two applications, 30–50% enriched oxygen is sufficient. To meet this requirement, Air Products (*105*, *106*) has developed a PSA process called "oxy-rich" which is very energy efficient. PSA compares very well with conventional methods, particularly when one is interested in smaller capacities, as seen in Table 4.

Nitrogen Production

High purity nitrogen can be produced by using carbon molecular sieves. This is significant as being the only commercial process which uses differences in the intraparticle diffusivity of adsorbate molecules as the basis for separation. Oxygen, which is smaller in size (critical diameter 2.8 Å) than nitrogen, diffuses much faster ($D/r^2 = 1.7 \times 10^{-4}\ s^{-1}$) in a carbon molecular sieve than nitrogen ($D/r^2 = 7 \times 10^{-6}\ s^{-1}$, 3.0 Å in critical diameter) and hence is selectively adsorbed. Figure 19 shows the uptake curves for oxygen and nitrogen on a commercial carbon molecular sieve. Nitrogen is the high pressure product. Oxygen (35–50%) is produced as the low pressure (extract) product during purge and blowdown. Typical operation conditions of nitrogen PSA are: cycle pressure, 4–0.1 atm; half cycle time, 1 min. With the advent of PSA, inert gas applications of nitrogen have increased. The major uses are:

Inert gas blanketing for safety purposes.
Purging process vessels of flammables.

TABLE 4
Comparison of PSA with Cryogenic Method

PSA	Cryogenic
Competitive below 30 t/day	Competitive above 30 t/day
Most readily makes comparatively low purity product	High purity product readily obtainable
Robust construction and operation	Sophisticated construction and operation
Low capital	High capital
Automatic operation comparatively straightforward	Automatic operation but difficult
Very rapid startup/shutdown	Takes several hours to come on-stream
Scales down well, up less well	Scales up well, down badly
95% pure	99+% pure

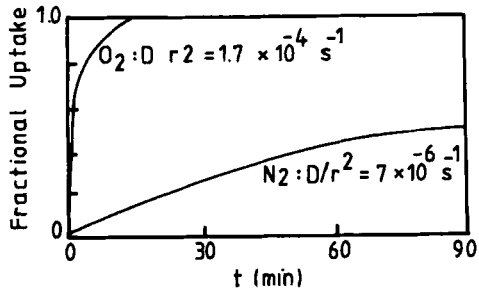

FIG. 19. Sorption uptake for N_2 and O_2 on carbon molecular sieve.

Inert flushing gas for petroleum tankers.
Food processing or preservation.
Inerting atmospheres for metal heat-treating.
Laboratory uses.

PSA is very competitive with the cryogenic process with its production rates of 2,000–30,000 ft^3/h (56–850 m^3/h). At its current rate of development, PSA promises to pose a serious challenge to the cryogenic process.

Attempts have been made in recent years to make an oxygen-selective zeolite by molecular engineering of the starting zeolite (*107*) in order to replace carbon molecular sieves. Zeolite 4A is modified by "dissolving" divalent iron and by partly exchanging sodium with potassium cations. The dissolution of Fe in the NaA results in the formation of terminal bonding such as —Si—O—Fe—, —Al—O—Fe—, —Si—O—Fe—, —Al—O—Fe—, etc. This type of bonding leads to a partial pore closure which in turn results in a slower diffusion of nitrogen. Efforts are being made to improve the processes for air separation (*107*, *108*) by using oxygen-selective zeolites based on the different diffusivities for N_2 and O_2.

A process for the simultaneous production of nitrogen and pure oxygen (99.7%) was developed (*109*) with an integrated PSA system having one zeolite molecular section and a carbon molecular sieve section. The feed air is first passed through the zeolite bed where nitorgen is removed. The product, which is a mixture of oxygen and argon, is passed through the carbon molecular sieve bed where argon is removed to yield pure oxygen.

Argon Recovery

Argon is a coproduct obtained during the production of N_2 or O_2 from air. In recent years, growing argon applications in ferrous and nonferrous industries and electronic component manufacturing plants have resulted in an increased demand for argon, necessitating alternative sources. An important source rich in argon is the purge gas from ammonia synthesis plants. The composition of hydrogen-depleted ammonia purge gas is as follows: hydrogen, 7–30% (by volume); nitrogen, 35–60%; argon, 6–12%; methane, 25–38%. The actual pressure (pressure ranges from 50 to 1900 psia) and composition of the purge gas depends on the design and operation of the ammonia plant as well as of the hydrogen recovery plant.

Processes currently in use for argon recovery from ammonia purge gas are based on three-column cryogenic systems. Krishnamurthy et al. (*110–112*) developed a PSA process for argon recovery from ammonia plant purge gas as an alternative to an all-cryogenic plant. The new process, called HARP (hybrid argon recovery process), employs a combination of PSA separation and cryogenic distillation. A novel aspect of this process is PSA removal of all of the methane and a major portion of N_2 in the feed gas.

A flow diagram of the HARP is given in Fig. 20. The feed gas enters a two-bed pressure swing adsorption system and is separated into two product streams; an argon-rich high pressure product and a methane-rich low pressure product. The PSA is operated so that the argon-rich product contains a very low concentration of methane.

The cryogenic section of the plant consists of a single column and a N_2 refrigeration circuit. The argon-rich product is fed to the column. In the column, pure liquid argon is produced as the bottom product and a hydrogen–nitrogen distillate is sent to the PSA at ambient temperature for

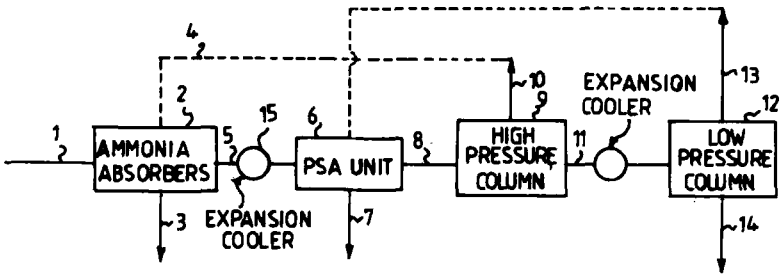

FIG. 20. Flow diagram of hybrid argon recovery process.

bed regeneration. During regeneration, it mixes with the methane-rich vent stream. The mixed vent and regeneration gas is sent back to the ammonia plant to recoup the fuel value. A detailed schematic diagram of the PSA unit is shown in Fig. 21. In addition to the two beds, the PSA unit consists of an equalization tank, a backfill tank, and a receiver for product, feed, vent, and regeneration gases. The PSA employs a commercially available type 5A zeolite molecular sieve as the adsorbent material. This sieve offers a high argon to methane selectivity. The equilibrium capacity for the 5A molecular sieve is in the following order: methane > nitrogen > argon > hydrogen.

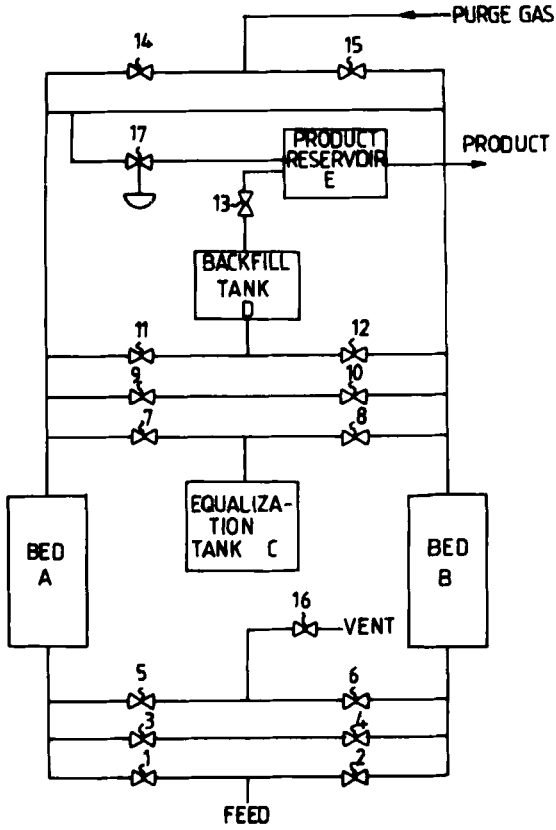

FIG. 21. A schematic diagram of the PSA unit of hybrid argon recovery process.

All of the hydrogen separates with the argon-rich stream, and N_2 distributes between the argon-rich and the methane-rich products. Other adsorbents which can also be used are zeolites 4A, 10X, and 13X, and sodium mordenite.

Hydrogen Recovery

PSA is widely used for the recovery of hydrogen from various streams. Hydrogen is not adsorbed on any commercial adsorbents and it can be obtained as a high purity product. Normally, 4A, 5A, or carbon molecular sieve adsorbents are used depending on the impurities to be removed. The main process development in hydrogen recovery was made by Union Carbide in the late 1970s wherein the use of a polybed (*113*, *114*) was introduced. This process takes advantage of a pressure equilization step and consists of 5 or more beds, even up to 10 beds as seen in Fig. 22. This is a very energy-efficient process. The recovery is about 85% as against 70–75% in a 4-bed process. The product purity can be as high as 99.9999%. The productivity is 10–29% more than in a simple PSA process.

The advantages of the PSA process can be appreciated by comparing it with the conventional method of hydrogen production by steam reforming of hydrocarbons which involves the following steps:

Desulfurization.
Steam reforming.

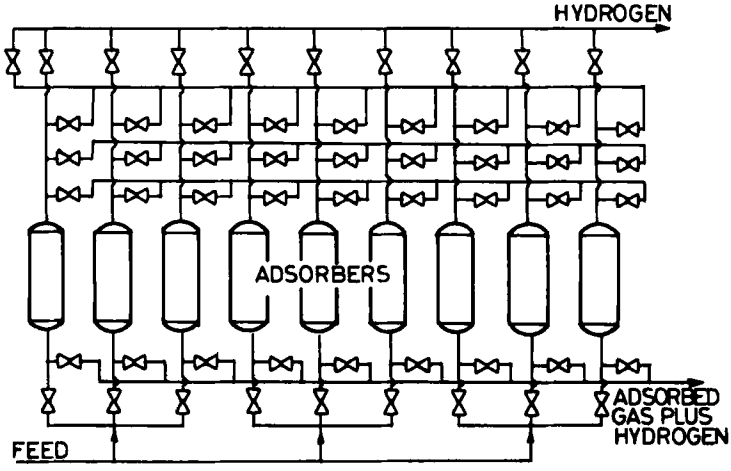

FIG. 22. A schematic diagram of polybed PSA process for hydrogen recovery.

High-temperature shift conversion.
Low-temperature shift conversion.
Co_2 removal by liquid adsorption.
Methanation.

In this process, 97–98% H_2 is normally obtained, with the residual impurity generally being methane. In the PSA process the last three steps are replaced by a PSA step where CO_2, CO, and CH_4 are removed in a single step. A final product of 99.9999% purity is obtained. Figure 23 shows a comparison of the two processes.

In the above PSA process, CO_2 is not recovered. Air Products has developed a polybed process (*20*, *115*, *116*) for the simultaneous recovery of hydrogen and carbon dioxide (Fig. 24). The crude hydrogen stream from the steam reformer contains carbon dioxide as a bulk impurity (15–25%). Recovery of the CO_2 as a by-product by a PSA process without sacrificing the purity and recovery of the hydrogen product can add significant value to the separation process. In addition, by resolving CO_2 as a product, the fuel value of the waste gas increases. This process can produce ultrapure H_2 (99.999+%) with 86–87% H_2 recovery with a CO_2 by-product (99.4% purity and 90+% recovery). The fuel gas stream produced by the process has a high Btu value with only 8–10% CO_2.

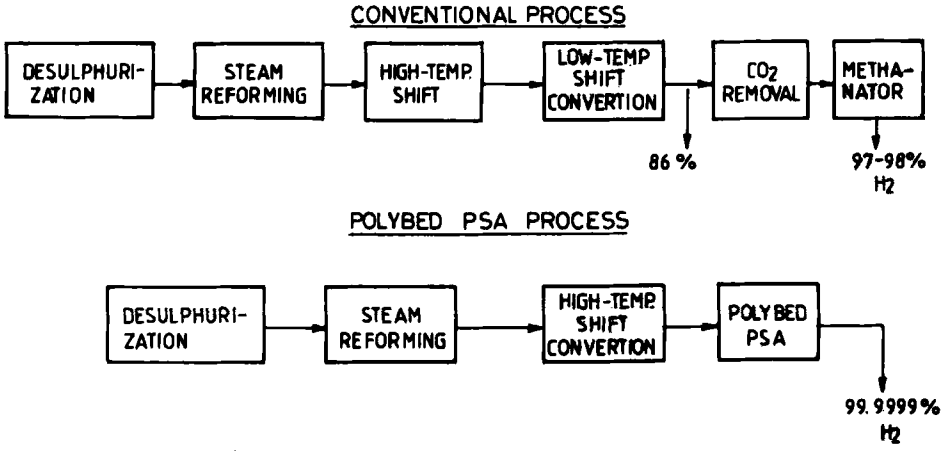

FIG. 23. Comparison of a PSA process with conventional method of hydrogen production via steam reforming.

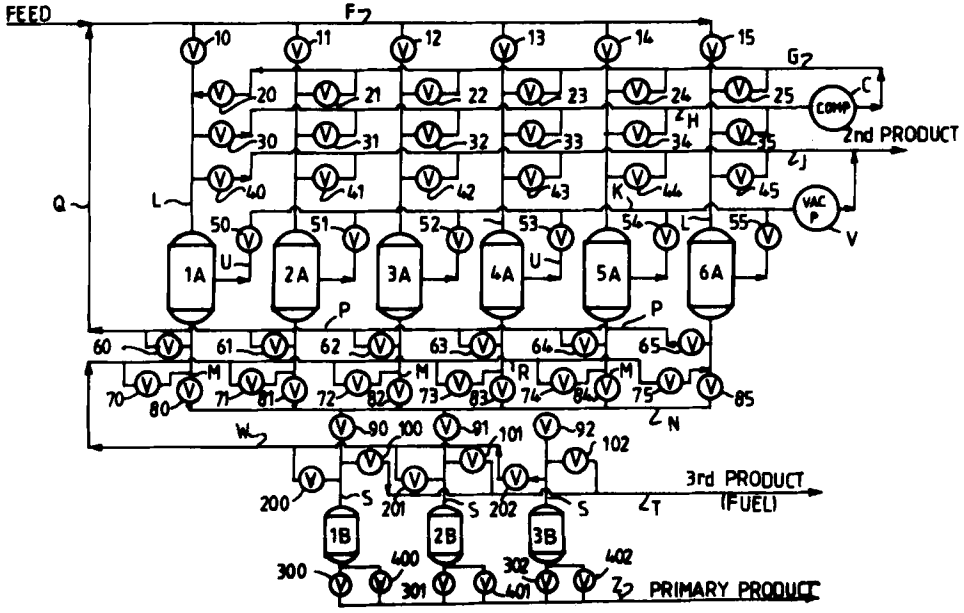

FIG. 24. Flow sheet of polybed pressure swing process for simultaneous recovery of hydrogen and carbon dioxide.

A novel commercial PSA process has been developed (*20*) for the production of ammonia synthesis gas by a modification of the above polybed PSA process. In this process, nitrogen from an external source is used to carry out the countercurrent purge and pressurization steps instead of using pure hydrogen product gas for these purposes. A substantial quantity of N_2 is introduced into the adsorber prior to the start of the adsorption step. The nitrogen is released from the adsorber as an H_2–N_2 mixture at the highest pressure during the adsorption step. It is possible to produce an ammonia synthesis gas containing a 3:1 molar ratio of H_2 and N_2 by appropriately designing the operating conditions of this process. The major advantage of this process is that the net H_2 recovery is substantially increased (93–94%) due to the absence of any H_2 purge loss. Another advantage is the recovery of high purity CO_2 (99%). It is claimed that this is an ideal process for urea manufacture applications where CO_2 and NH_3 are reacted to form urea.

Some of the other uses of polybed PSA are:

Refinery H_2 upgrading as a substitute for the cryogenic process.
Ammonia loop vent stream.

Ethylene plant off-gas.
Meeting the hydrogen requirement in coal gasification/liquefaction.

Normal Paraffin Separation

Normal paraffin separation was one of the earliest PSA applications, and it has been widely described in the literature. PSA has been successfully employed in Union Carbide's Isosiv process for the separation of *n*-alkane (C_3–C_5) from branched/cyclic paraffins.

Methane Recovery

Methane is found (20 to 50%) in combination with carbon dioxide and nitrogen in a variety of situations, e.g., in some natural gas reservoirs (50% CO_2), in the effluent gas from oil wells undergoing CO_2 flooding for enhanced oil recovery (20–80% CO_2), and in municipal and industrial landfill gases (40–60% CO_2). It is desirable to recover CH_4 either as a medium-energy or a high-energy gas for its use as a fuel or pipeline quality methane stream. PSA has made substantial progress in the recovery of CH_4 from landfill gas (*117–119*). The anaerobic breakdown of a carbohydrate in a landfill produces methane and carbon dioxide. Landfill gas (LFG) also contain other impurities (*118*, *119*) which depend on the nature of the refuse. LFG is recovered by drilling wells into a landfill and applying a vacuum. Membrane, absorption, and adsorption processes have been used for methane recovery. Whereas the membrane and absorption processes operate at higher pressures (1.7–5.5 MPa) with 70–90% methane recovery, PSA operates at lower pressures (0.34–1.03 MPa). Both kinetic and equilibrium-based separations are used in PSA. Air Products (*119*) has developed a commercial process which removes all the chemical impurities to below 1 ppm with 90% methane purity and 96% overall recovery. This process is a composite of a thermal swing and a pressure swing adsorption steps. The undesirable impurities are eliminated in the thermal swing adsorption step (TSA). Methane is produced by the PSA step. In TSA, widepore iodized activated carbon is used as both an adsorbent and a catalyst (*118*). Zeolites and carbon molecular sieves can both be used for methane recovery.

Another process (*120*) for the simultaneous production of CO_2 and CH_4 has been reported in which the recoveries of both components are very high (99.0%). This process uses a CO_2 selective zeolite adsorbent.

Enrichment of methane by using carbon molecular sieves is also reported from firedamp where it is found (27–50%) in combination with N_2, O_2,

and argon (*15*). The possibility of using silicalite for such application has been shown recently (*66*, *67*).

Carbon Monoxide Production

Gases containing carbon monoxide are commonly exhausted from many steel mills. For example, a typical composition of Linz–Donauwitz converter gas is CO = 75–87%, CO_2 = 3–8%, N_2, H_2 = 1–6%, O_2 = 80–90 ppm, COS = 4–6%, H_2 = 2 ppm, and NO = 4–6%. Recovery of carbon monoxide from these provides an effective means of resource utilization because CO can be used as a raw material for C_1 chemistry. Wet processes, such as the copper salt scrubbing process of the liquefication separation process, were earlier used for CO separation. However, a carbon monoxide pressure-induced selective adsorption process was recently developed jointly by Kawasaka Steel Corp. and Osaka Oxygen Industries Ltd. by making use of adsorbent Na-mordenite (*121*). This process consists of two stages. In the first stage, carbon dioxide is removed by using PSA with activated carbon as an adsorbent. In the second stage, CO is recovered from its mixture with N_2 by using Na-mordenite. Product gas is recovered by evacuating the bed. The adsorption isotherms of CO and N_2 on this adsorbent are shown in Fig. 25.

A carbon monoxide selective adsorbent was also developed by immersing the activated carbon particles in an acidic solution of $CuCl_2$ and then

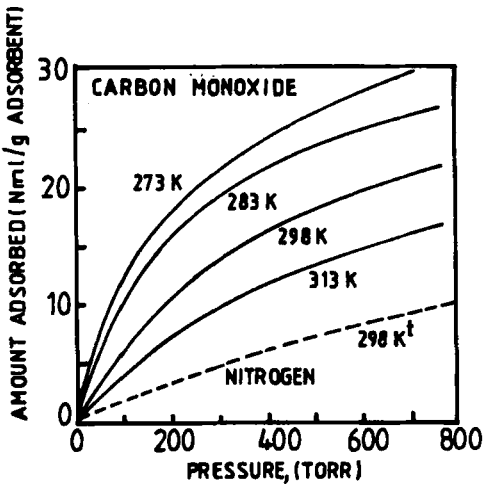

FIG. 25. Adsorption isotherms of nitrogen and carbon monoxide on Na-type mordenite.

evacuating the liquid phase. This adsorbent selectively adsorbs CO at room temperature and desorbs it completely at 393 K or by evacuating to 0.4 torr at room temperature (*122*). Mitsubishi Kakoki Kaisha Ltd. reported (*121*) a PSA process for CO recovery which uses this adsorbent.

Ozone Enrichment

Ozone is preferentially adsorbed on silica gel and zeolite from its mixtures with oxygen or nitrogen. Processes using silica gel/zeolite adsorbent for ozone enrichment from oxygen and nitrogen have been reported (*15*). Ozone enrichment from oxygen is relatively simple, with two adsorbent beds operating alternately. The flow sheet for ozone enrichment from a nitrogen stream is given in Fig. 26. In the first step, nitrogen is largely removed by adsorption from the compressed (maximum 6 bar) air stream. The oxygen-rich stream then flows to the ozonizer (pressure < 2 bar) where ozone is produced (4 vol%). This is then compressed and passed over the regenerated adsorber where ozone and the residual nitrogen are adsorbed, and the oxygen-rich gas returns to the ozonizer. This step is continued until the adsorber bed reaches a breakthrough stage. In the last step, nitrogen and ozone are recovered by depressurization and oxygen flushing.

Miscellaneous Developments

The PSA process is relatively simple, requiring only compressors, occasionally vacuum pumps, and a few switching valves. The adsorbent life is very high, necessitating its replacement largely due to attrition. It has the advantage of having the capability of producing the gas at any desired

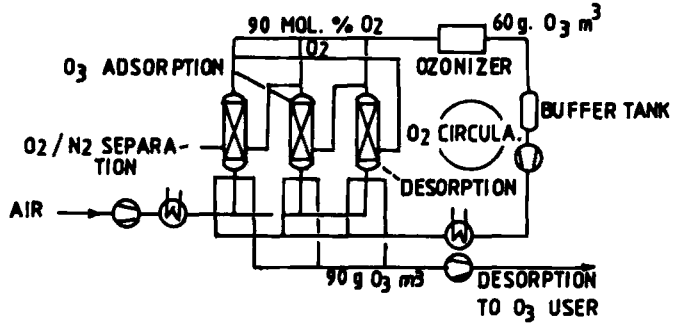

FIG. 26. Flow sheet of a pressure swing process for ozone enrichment.

purity with minor modifications of the operating steps. As a result, the potential for PSA application has been explored in various fields. Some of these are mentioned below:

NO_x removal from nitric acid waste gases.
Propene/propane, ethene/ethane, and butene/butane separations.
Ethane/methane separation.
Acetylene/ethene separation.

Pressure Swing Parametric Pumping (PSPP) or Rapid PSA (RPSA)

Pressure swing parametric pumping or rapid PSA was developed to minimize process complexity and investment at the expense of product recovery. The term "parametric pumping" was coined by Wilhelm (*123*) who described an adsorption-based separation process involving reversing flows. When the flow is in one direction, a parameter, such as temperature or pressure, which influences adsorptivity, is at one value while the parameter is changed to another value when the flow is in the opposite direction. Such a process creates separation between components with different adsorptivities. PSPP exists in both single-bed and multibed processes. Schematic diagrams of these processes are shown in Figs. 27 and 28. The feed gas under pressure is supplied in pulses of up to about a second in length from a compressor and a surge tank. The pulse is controlled by a solenoid valve and a timer. During this feed pulse, the exhaust solenoid valve is closed. Following the feed pulse, both valves at the feed end are closed for about 0.5 to 3 s; this period is called the delay. Next, the solenoid valve on the exhaust or the purge line opens for a period of about 5 to 20 s. Since the pressure in this line is maintained below that in the feed line, reverse flow of gas from the bed occurs. Finally, another delay period with both solenoid valves closed is used in some cases. Its length is generally less than 1 s. However, while pressures and flow directions are fluctuating substantially at the feed end of the bed, a continuous

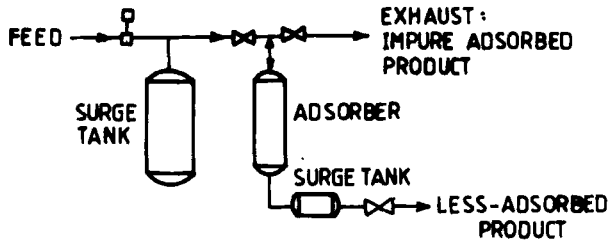

FIG. 27. Flow sheet of one-bed pressure swing parametric pumping.

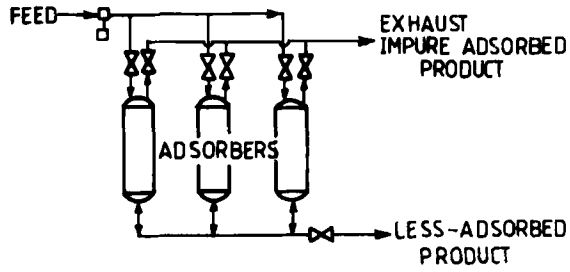

FIG. 28. Flow sheet of three-bed pressure swing parametric pumping.

flow emerges from the product end and through a small surge tank. This flow is enriched in less-adsorbed components; in the case of air separation, the product typically consists of 90 to 95% O_2, with the balance Ar and a small amount of N_2. The multibed process is similar to the single-bed process. The multibed process usually produces somewhat higher, less-adsorbed product pressures and lighter, higher, less-adsorbed product recoveries compared to the single-bed process. PSPP, like polybed PSA, represents quite a different approach to improving the basic PSA process.

PSPP has been commercialized for the production of oxygen and for the recovery and recycle of ethylene and a small amount of chlorocarbons (the adsorbed stream) to an ethylene-chlorination process while purging nitrogen (the less-adsorbed component) from the process.

SUMMARY

The pressure swing adsorption process as a technique to separate multicomponent gaseous mixtures is reviewed. The various types of adsorbents used for this purpose are described in detail. Special attention has been paid to the potential uses of a new generation of adsorbents: molecular sieves. The most widely accepted theories for the prediction of multicomponent adsorption isotherms from single component data are briefly presented. Commercial applications of the PSA process are extensively discussed.

NOTATION

$\ddot{a}_i$	partial molar surface area of i
A	surface area of adsorbent
b_i, k	Henry's law constant for i
C	amount adsorbed
C_A	amount adsorbed for Component A
ΔG_i°	standard state free energy of adsorption of pure i (J/mol)

m	number of molecules of sorbate
n_i^s	number of moles of i in adsorbed phase
$n_i^{s,\infty}$	limiting value of n
n_m^s	total number of moles of mixture in surface phase
$n_m^{s,\infty}$	limiting value of n_m^s
p	pressure of pure gas in equilibrium with its adsorbed phase
P	total pressure of mixture in equilibrium with its adsorbed phase
R	gas constant
T	temperature of adsorption system
V	free volume of zeolitic cavity
V_{mix}	total amount adsorbed for mixture
$V_i^\circ(\Pi)$	amount of pure component i adsorbed at spreading pressure, Π
x_A, x_B	mole fraction of Components A and B in gas phase
x_i	mole fraction of i in vacancy-free adsorbed phase
x_i^s	mole fraction of i in adsorbed-phase vacancy solution
y_A, y_B	mole fraction of Components A and B in adsorbed phase
y_i	mole fraction of i in vacancy-free vapor phase
α_{ij}	parameter describing nonideality in adsorbed phase induced by interaction between species i and j
β	molecular volume of the sorbate
ϕ_i	fugacity coefficient of i in bulk gas mixture
γ_i	activity coefficient of i in adsorbed-phase vacancy solution
Λ_{i3}	Wilson parameter for interaction between component i and vacancy. Subscript 3 refers to vacancy
Π	spreading pressure of adsorbed mixture
θ	fractional coverage

Superscripts

s	surface phase value
∞	value at maximum adsorption limit
$^\circ$	standard state value

Subscripts

1, 2	component 1, 2
i, j, k	component i, j, k
A, B	Component A, B
mix	mixture
v	vacancy

Acknowledgments

The authors are grateful to Dr. T. S. R. Prasada Rao for useful discussions and to Dr. I. S. Bharadwaj, Director, R & D, for his keen interest and permission to publish this article.

REFERENCES

1. S. Sircar, U.S.—India Cooperative Seminar on Chemical Engineering Education: Curricula for Future, held at Indian Institute of Sciences, Bangalore, India, 1988.
2. C. W. Skarstrom, in *Separation Science,* Vol. II, (N. N. Li, ed.), CRC Press, Boca Raton, Florida, 1972, p. 95.
3. W. N. Chen and R. T. Yang, in *Recent Developments in Separation Science,* Vol. IX, (N. N. Li and J. M. Calo, eds.), CRC Press, Boca Raton, Florida, 1984.
4. C. N. Kenny and N. F. Kirkby, *Zeolites: Science and Technology* (F. Ribeiro, A. E. Rodriques, L. D. Rollman, and C. Naccache, eds.), Martins Nijhoff, The Hague, 1984.
5. H. Lee and D. E. Stahl, *AIChE Symp. Ser., 69*(134), 1 (1973).
6. G. R. Landolt and G. T. Kerr, *Sep. Purif. Methods, 2,* 283 (1973).
7. A. Mersmann, U. Munstermann, and J. Schadl, *Ger. Chem. Eng., 7,* 137 (1984).
8. M. S. Ray, *Sep. Sci. Technol., 18,* 95 (1983).
9. D. Tondeur and P. C. Wankat, *Sep. Purif. Methods, 14,* 157 (1985).
10. P. C. Wankat, *Large-Scale Adsorption and Chromatography,* Vol. I, CRC Press, Boca Raton, Florida, 1986.
11. G. E. Keller II, in *Industrial Gas Separations* (ACS Symposium Series), (T. E. Whyte Jr., C. M. Yon, and E. H. Wagener, eds.,), American Chemistry Society, Washington, D.C., 1983, p. 223.
12. G. E. Keller II, in *Handbook of Separation Process Technology* (R. W. Rousseau, ed.), Wiley, New York, 1987.
13. R. T. Yang, *Gas Separation by Adsorption Process,* Butterworths, London, 1986.
14. D. M. Ruthven, *Principles of Adsorption and Adsorption Process,* Wiley, New York, 1984.
15. R. Richter, K.-B. Harder, K. Oblauch, and H. Juntgen, *Ger. Chem. Eng., 8,* 203 (1985).
16. C. W. Skarstrom, US Patent 2,944,627 (1960).
17. C. W. Skarstrom, *Ann. N. Y. Acad. Sci., 72*(13), 751 (1959).
18. N. H. Berlin, US Patent 3,280,536 (1966).
19. J. C. Davis, *Chem. Eng., 16,* 88 (October 1972).
20. S. Sircar, in *Recent Advances in Chemical Engineering* (D. N. Saraf and D. Kunzru, eds.), Tata McGraw-Hill, New Delhi, 1989.
21. D. W. Breck, *Zeolite Molecular Sieves,* Wiley-Interscience, New York, 1978.
22. R. Szostak, *Molecular Sieves: Principles of Synthesis and Identification,* 1989.
23. R. M. Barrer, *Zeolite and Clay Minerals as Sorbents and Molecular Sieves,* Academic, New York, 1978.
24. E. M. Flanigen, *Pure Appl. Chem., 52,* 2191 (1980).
25. R. V. Jasra and S. G. T. Bhat, *Sep. Sci. Technol., 23,* 945 (1988).
26. R. A. Anderson and J. D. Sherman, *AIChE Symp. Ser., 292*(80), 118 (1984).
27. H. Juntgen, *Carbon, 15,* 273 (1977).
28. H. Juntgen, K. Knoblauch, and H. J. Schroter, *Ber. Bunsengesellschaft Phys. Chem., 79*(9), 824 (1979).
29. K. Kawazoe, M. Suzuki, and K. Chihara, *J. Chem. Eng. Jpn., 7,* 151 (1974).

30. P. L. Walker Jr., L. G. Austin, and S. P. Nandi, in *Chemistry and Physics of Carbon,* Vol. 2 (P. L. Walker Jr., ed.), Dekker, New York, 1966.
31. H. Juntgen, K. Knoblauch, and H. Harder, *Fuel, 60,* 817 (1981).
32. D. H. T. Spencer, in *Porous Carbon Solids* (R. L. Bond, ed.), Academic, New York, 1967, p. 87.
33. K. Knoblauch, *Chem. Eng. (New York) 85*(25), 87 (1978).
34. H. B. Nataraj, M.Tech. Thesis Submitted to Department of Chemical Engineering, Indian Institute of Technology, Bombay, 1990.
35. A. Tsuruizumi, *Bull. Chem. Soc. Jpn., 34*(7), 1457 (1961).
36. J. E. Metcalfe III, M. Kawahata, and P. L. Walker, *Fuel, 42*(3), 233 (1963).
37. J. E. Metcalfe III, Ph.D. Thesis, Pennsylvania State University, University Park, Pennsylvania, 1965.
38. T. G. Lamond, J. E. Metcalfe III, and P. L. Walker Jr., *Carbon, 3,* 59 (1965).
39. S. Ida, K. Tatsumoto, and M. Matsuoka, Japanese Patent 61 251,507.
40. H. Juntgen, *Carbon, 15*(3), 281 (1981).
41. N. D. Drozolina, V. G. Volkova, and N. O. Bulgakova, *Khim. Tverd. Topl., 3,* 30 (1975).
42. R. J. Grant, US Patent 3,884,830 (1975).
43. M. Jozefczak-Ihler, M. Francois, and H. Guerin, *C. R. Hebd. Seances Acad. Sci., Ser. C, 20,* 280 (1975).
44. P. N. Satyendra and P. L. Walker Jr., *Fuel, 54*(3), 169 (1975).
45. J. Siedlewski and R. Majewski, *Koks, Smola, Gaz, 20*(7–8), 206 (1975).
46. S. V. Moore and D. L. Trimm, *Carbon, 15,* 177 (1977).
47. S. Spitzer, J. Hrncir, S. Sindler, and J. Havlicek, Czechoslovakian Patent 224,299 (1978).
48. Agency of Industrial Science and Technology, Japanese Patent 80 71,615 (1980).
49. R. C. Bansal, T. L. Dhami, and Satyaprakash, *Indian J. Chem., 19A,* 1146 (1980).
50. H. Kitagawa and N. Yuki, *Nenryo Kyokai-Shi, 60*(645), 46 (1981).
51. H. Kitagawa and N. Yuki, *Ibid., 61*(657), 1152 (1982).
52. K. Ishibashi and R. Kobayashi, *Ibid., 62*(669), 70 (1983).
53. S. Spitzer, V. Biba, and J. Hrncir, *Chem. Zvesti, 37*(1), 23 (1983).
54. Japan Oxygen Co., Ltd., Japanese Patent 59 230,637.
55. F. Sutt Robert, European Patent 102,902.
56. M. Kashiwase, Japanese Patent 61 191,510.
57. K. Knoblauch, German Patent 3,618,426.
58. E. M. Flanigen et al., US Patent 4,104,294.
59. G. R. Landolt, US Patent 3,702,886.
60. S. T. Wilson, B. M. Lok, and E. M. Flanigen, US Patent 4,310,440 (1982).
61. B. M. Lok, C. A. Mezzina, R. L. Patton, R. T. Gajek, T. R. Cannan, and E. M. Flanigen, US Patent 4,440,871 (1984).
62. S. T. Wilson and E. M. Flanigen, US Patent 4,567,029 (1986).
63. M. E. Davis, C. Saldarriaga, C. Montes, J. Garces, and C. Crowder, *Zeolites, 8,* 362 (1988).
64. J. Wang, S. Feng, and R. Xu, *J. Chem. Soc., Chem. Commun., (5),* 265 (1989).
65. G. Harvey and W. M. Meier, in *Zeolites: Facts, Figures, Future* (P. A. Jacobs and R. A. Van Santen, eds.), Elsevier, Amsterdam, 1989, p. 41.
66. P. Grahm, A. D. Hughes, and L. V. C. Rees, *Purif. Sep. Methods, 3,* 56 (1989).
67. R. V. Jasra and L. V. C. Rees, Unpublished Results.
68. E. F. Vansant, in *Innovation in Zeolite Material Science* (P. J. Grobet, ed.), Elsevier, Amsterdam, 1988, p. 143.

69. R. M. Barrer, E. F. Vansant, and G. Peeters, *J. Chem. Soc., Faraday Trans. 1, 74,* 1871 (1978).
70. A. Thijs, G. Peeters, E. F. Vansant, I. Verhaert, and P. De Bievre, *Ibid., 79,* 2821, 2835 (1983).
71. A. Thijs, G. Peeters, E. F. Vansant, and I. Verhaert, *Ibid., 82,* 963 (1986).
72. M. Niwa, S. Kato, T. Hattori, and Y. Murakami, *Ibid., 80,* 3135 (1984).
73. E. F. Vansant, P. De Bievre, G. Peeters, A. Thijs, and I. Verhaert, *Eur. Appl. Res. Rep.—Nucl. Sci. Technol., 4,* 893 (1982).
74. M. Niwa, K. Yamazaki, and Y. Murakami, *Chem. Lett., (3),* 441 (1989).
75. R. V. Jasra and S. G. T. Bhat, *Ind. Eng. Chem. Res., 26,* 2546 (1987).
76. N. V. Choudary, R. V. Jasra, and S. G. T. Bhat, Unpublished Results.
77. E. D. Markham and A. F. Benton, *J. Am. Chem. Soc., 53,* 497 (1931).
78. D. B. Broughton, *Ind. Eng. Chem., 40,* 1506 (1948).
79. C. Kemball, E. K. Rideal, and E. A. Guggenheim, *Trans. Faraday Soc., 44,* 948 (1948).
80. S. G. T. Bhat, "Physical Adsorption from Mixtures of Gases," Ph.D. Thesis Submitted to Chemistry Department, Indian Institute of Science, Bangalore, 1971.
81. S. G. T. Bhat, R. V. Jasra, and N. V. Choudary, Unpublished Results.
82. C. M. Yon and P. H. Turnock, *AIChE Symp. Ser., 67*(117), 75 (1971).
83. A. L. Myers and J. M. Prausnitz, *AIChE J., 11,* 121 (1965).
84. D. Valenzuela and A. L. Myers, *Sep. Purif. Methods, 13,* 153 (1984).
85. S. G. T. Bhat, and K. S. Narayan, *Indian J. Chem., 20A,* 1167 (1981).
86. E. Costa, J. L. Sotelo, G. Calleja, and C. Marron, *AIChE J., 27,* 5 (1981).
87. S. Suwanayuen and R. P. Danner, *Ibid., 26,* 68, 76 (1980).
88. S. H. Hyun and R. P. Danner, *J. Chem. Eng. Data, 27,* 196 (1982).
89. T. W. Cochran, R. L. Kabel, and R. P. Danner, *AIChE J., 31,* 268, 2075 (1985).
90. D. M. Ruthven and K. F. Loughlin, *Chem. Eng. Sci., 28,* 701 (1973).
91. K. Fiedler, G. Finger, U. Noack, and M. Bulow, *Z. Phys. Chem. (Liepzig), 268,* 881 (1987).
92. G. A. Sorial, W. H. Granville, and W. O. Daly, *Chem. Eng. Sci., 38,* 1517 (1983).
93. H. W. McRobbie, US Patent 3,140,931 (1964).
94. D. W. McKee, US Patent 3,140,932 (1964).
95. R. V. Jasra, N. V. Choudary, and S. G. T. Bhat, Unpublished Results.
96. S. Sircar, European Patent 128,545 (1984).
97. C. G. Coe and S. M. Kuznicki, European Patent 109,063 (1984).
98. R. J. Neddenriep, *J. Colloid Interface Sci., 28,* 293 (1968).
99. C. G. Coe, S. M. Kuznicki, R. Srinivasan, and R. J. Jenkins, in *Perspectives in Molecular Sieve Sciences* (ACS Symposium Series, 368), (W. H. Flank and T. E. Whyte Jr., eds.), American Chemical Society, Washington, D.C., 1988, p. 478.
100. G. E. Miller, *AIChE Symp. Ser., 259,* 28 (1987).
101. G. E. Miller, K. S. Knaebel, and K. G. Ikels, *AIChE J., 33*(2), 194 (1987).
102. D. M. Ruthven, *Ibid., 22,* 753 (1976).
103. K. A. M. Wester, Ph.D. Thesis Submitted to Department of Chemical Engineering, Royal Institute of Technology, Stockholm, 1987.
104. S. G. T. Bhat and K. S. Narayan, *Indian J. Chem., 16A,* 294 (1978).
105. W. C. Kartz and S. Sircar, US Patent 4,685,939 (1987).
106. S. Sircar and W. C. Kartz, *Sep. Sci. Technol., 23*(4&5), 437 (1988).
107. J. Izumi et al., European Patent 40,935 (1981).
108. H. S. Shin and K. S. Kneabel, *AIChE J., 34,* 1409 (1988).
109. BOC Ltd., UK Patent 2,011,272 (1979).

110. R. Krishnamurthy, S. L. Lerner, and D. L. MacLean, *Gas Sep. Purif., 1*(1), 16 (1987).
111. R. Krishnamurthy and S. L. Lerner, *AIChE Symp. Ser., 84*(264), 84 (1988).
112. D. L. MacLean, R. Krishnamurthy, and S. L. Lerner, US Patent 4,689,062 (1987).
113. R. T. Cassidy, in *Adsorption and Ion Exchange with Synthetic Zeolites* (ACS Symposium Series, 135), (W. H. Flank, ed.), American Chemical Society, Washington, D.C., 1980, p. 247.
114. J. L. Heck, *Oil Gas J., 11,* 122 (February 1980).
115. S. Sircar, US Patent 4,171, 206 (1979).
116. W. C. Kratz, D. L. Rarig, and J. M. Pietrantonio, *AIChE Symp. Ser., 84*(264), 36 (1988).
117. S. Sircar, *Sep. Sci. Technol., 23,* 519 (1988).
118. H. Schilling and W. Hinz, in *New Directions in Sorption Technology* (G. E. Keller II and R. T. Yang, eds.), Butterworths, London, 1989, p. 75.
119. R. Kumar and J. K. van Sloun, *Chem. Eng. Prog.*, p. 75 (January 1989).
120. S. Sircar and J. W. Zondlo, US Patent 4,077,779 (1978).
121. M. Suzuki, *AIChE Symp. Ser., 84*(264), 119 (1988).
122. K. Tajima and Y. Osada, US Patent 4,783,433 (1988).
123. R. H. Wilhelm, *Ind. Eng. Chem., Fundam., 5,* 141 (1966).

Received by editor September 17, 1990